Nitrate production beneath a High Arctic glacier, Svalbard

Wynn, P.M[a*], Hodson, A.J[a], Heaton, T.H.E[b], and Chenery, S.R.[b]

[a] *Department of Geography, University of Sheffield, Winter St., Sheffield S10 2TN, UK*

[b] *British Geological Survey, Keyworth, Nottingham NG12 5GG, UK*

Abstract

Natural environmental isotopes of nitrate and ammonium are used in conjunction with major ion chemistry and hydrological data to establish controls upon the biogeochemical cycling of nitrogen beneath a High Arctic polythermal glacier (Midtre Lovénbreen). Here, high nitrate concentrations in subglacial meltwaters suggest that the subglacial environment may be furnishing nitrate in excess of that released from the snowpack and glacier ice. Isotopic values of $\delta^{18}O_{NO3}$ suggest the provenance of such excess nitrate to be microbial in origin and $\delta^{15}N_{NO3}$ indicates the source nitrogen compounds to have high $\delta^{15}N$ values relative to supraglacial runoff. We address the nitrification of supraglacial ammonium, the mineralization of organic nitrogen and the oxidation of geologic ammonium as potential sources of this additional nitrate. Mass fluxes of N compounds in a subglacial river and their $\delta^{15}N$ ratios indicate that the nitrification of supraglacial ammonium delivered to the glacier bed can account for much, but not all, of the excess nitrate. The additional source most likely involves the mineralization of organic nitrogen, although $\delta^{15}N$ values in rock samples suggest that the dissolution of rock-derived ammonium cannot be discounted if large fractionation effects occur during dissolution. Our results therefore agree with previous catchment scale mass balance studies at the site, which report a major internal loss of NH_4^+ from the snowpack following melt. However, at the catchment scale, the NH_4^+ loss is greater than the excess of NO_3^- observed in runoff, indicating that microbial assimilation of ammonia into organic matter in a range of other habitats is also likely. The identification of NH_4^+ assimilation and nitrification further highlights the non-conservative behaviour of nitrogen in glacial environments and testifies to the importance of microbially-mediated reactions in the biogeochemical cycling of nitrogen in an environment that has, until recently, been regarded as biologically inert.

[*] *Corresponding Author: School of Geography, Earth and Environmental Sciences, University of Birmingham, Edgbaston, Birmingham, B15 2TT. Tel: +44 121 414 5544; Fax: +44 121 414 5528; e-mail: p.m.wynn@bham.ac.uk*

Key words: Nitrogen isotopes, Oxygen isotopes, Subglacial drainage, Geologic nitrogen, Microbiological activity

1. Introduction

Solute acquisition by glacial meltwaters takes place at the bed of glaciers during transit through distributed and channelised drainage systems (eg. Raiswell, 1984; Tranter et al. 1993, 1996, 1997). The distributed system pertains to hydrological flowpaths conveying water under high pressure with long residence times and high rock/water contact ratios. Channelised drainage networks however follow discrete flowpaths, represent low pressure hydrological systems and evacuate large volumes of water rapidly from beneath the glacier. The spatial and temporal evolution between the two systems depends upon the flux of meltwater to the glacier bed, whereby high inputs of supraglacial meltwater raise the basal water pressure and encourage a spatial re-organisation of the drainage system such that the channelised system evolves at the expense of the distributed configuration (e.g. Richards et al. 1996; Nienow et al. 1998). Such hydrological forcing of subglacial drainage evolution at predominantly cold, polythermal glaciers can be rapid and closely coupled to the dynamics of glacier movement (Copland et al. 2003; Nuttall and Hodgkins, 2005; Rippin et al., 2005; Bingham et al. 2006). A concomitant change in the hydrochemistry of subglacial runoff accompanies this transition and can be manifest as a rapid switch in the chemical properties of the melt water (Copland et al. 2003; Wynn et al. 2006). Due to extensive rock/water contact and weathering reactions, high pressure distributed drainage configurations encourage high total dissolved ion loads and low concentrations of atmospheric gases in solution. However, during the hydrological evolution of the subglacial drainage system, the development of channelised flow paths conveying large volumes of meltwater subjected to only limited rock/water contact means that waters are more dilute and dissolved gases in solution exceed the capacity of oxygen consuming reactions at the glacier bed (e.g. Tranter et al, 2002). However, since the presence of microbiological activity within ice and subglacial sediments is now widely acknowledged (Bhatia et al. 2006; Foght et al. 2004; Mader et al. 2006; Sharp et al. 1999, Skidmore et al. 2000; Tranter et al. 2005; Welker et al. 2002), researchers are increasingly aware that acquisition of solute in sediments at distance from such channels may be effectively decoupled from inorganic controls of gas supply and rock/water contact ratios. Atmospheric gas supplies thus become depleted in the distributed drainage system, and so the use of alternative oxidising agents by microbial populations is required to drive further solute

64 acquisition under anoxic conditions (Bottrell and Tranter, 2002; Wadham et al. 2004; Wynn
65 et al. 2006). Despite this increased understanding, the degree to which such biotic solute
66 acquisition is governed by the evolution of the subglacial hydrological system remains largely
67 unknown (Tranter et al. 2005; Wynn et al. 2006; Hodson et al. In Press).

68

69 The NO_3^- ion represents one of the more readily available electron donors under reducing
70 conditions, and so should be highly sensitive to the redox evolution of the subglacial
71 hydrological system (Tranter et al. 1994; Wynn et al. 2006; Hodson et al. In Press). Thus,
72 during the early stages of summer ablation, subglacial meltwater in the distributed drainage
73 configuration includes pockets of local anoxia that are characterised by nitrogen isotopic
74 values that are diagnostic of microbial denitrification (Wynn et al. 2006). However, later in
75 the summer, when most meltwaters are conveyed through the aerated low pressure
76 channelised system, concentrations of nitrate and NO_3^-/Cl^- ratios in the subglacial meltwaters
77 increase significantly, implying the presence of an additional source of nitrate to the
78 subglacial drainage system. Hodson et al. (2005a) and Hodson (2006), show that some form
79 of NO_3^- production must take place, because annual NO_3^- yields exceed inputs in a number of
80 glacial environments, (including Midtre Lovénbreen). Such "excess NO_3^-" is also implicit in
81 meltwater hydrochemical studies of temperate glacier basins in the European Alps (Tockner
82 et al. 2002) and cold-based glaciers of the maritime Antarctic (Caulkett and Ellis-Evans,
83 1997; Hodson, 2006) although its precise source has yet to be identified.

84

85 An appreciation of the manner in which glaciers regulate the biogeochemical cycling of
86 nutrients and thereby impact upon the productivity of neighbouring freshwater and marine
87 ecosystems demands a better understanding of the non-conservative behaviour of nitrogen
88 and other nutrients in glacial environments on a sub-annual basis. Here, we build upon earlier
89 annual mass balance studies of nitrogen and trace the provenance and dynamics of 'excess'
90 NO_3^- production in the subglacial environment of a high Arctic glacier at a seasonal time
91 scale. In so doing, major ion chemistry (NO_3^-, NH_4^+ and Cl^-) and environmental isotopes of
92 $\delta^{15}N_{NO3}$, $\delta^{18}O_{NO3}$ and $\delta^{15}N_{NH4}$ in pre-melt snow, meltwater, organic matter and whole rock
93 samples are presented from Midtre Lovénbreen, Svalbard.

94

95 **2. Methodology**

96 *2.1. Field site and sampling*

97 Midtre Lovénbreen is a high Arctic polythermal glacier situated on the Brøggerhalvøya
98 peninsula in North West Spitsbergen (78.53ºN and 12.04ºE). The geology of the peninsula
99 includes basement rocks belonging to the Lower, Middle and Upper Proterozoic that are
100 situated beneath the glacier and predominantly composed of phyllites and beds of quartzite
101 (Hjelle, 1993). To the south of the phyllites are more strongly metamorphosed rocks that
102 include mica schists and beds of marble beneath the accumulation area of the glacier (Hjelle,
103 1993).

104 The glacier is up to 180m thick and two thirds of the ice is at the pressure melting point,
105 thereby supporting an extensive subglacial drainage system (Rippin et al. 2003). Bulk
106 meltwater runoff is conveyed towards the adjacent fjord of Kongsfjorden via two main
107 proglacial melt channels draining the lateral margins of the glacier (Hodson et al. 2005b)
108 (Figure 1). Meltwater accesses the bed of the glacier via moulins in the accumulation area,
109 later emerging as a pressurised subglacial upwelling (MLSG) at the terminus of the glacier
110 (Irvine-Fynn et al. 2005) (Figure 1), the dynamics of which are described by Rippin et al.
111 (2003) and Hodson et al. (2005a). Since subglacial meltwaters are characteristically sub-oxic
112 early in the ablation season, but well aerated thereafter, we have separated our observation
113 periods accordingly (see Wynn et al. 2006). Hereafter, early (sub-oxic) and later (oxic)
114 subglacial runoff will be referred to as the "initial" and "principal" runoff phases respectively,
115 reflecting the relative importance of the runoff fluxes associated with each period. During
116 summer 2002, samples of subglacial runoff were collected directly from the upwelling,
117 although during summer 2003, the upwelling changed location during the melt season causing
118 a small supraglacial stream to enter the subglacial runoff before sampling was possible, thus
119 confounding direct geochemical characterisation (Figure 1 and Table 1). Major ion
120 characterisation and data sourced from gauging stations installed on the two major bulk
121 meltwater channels draining the proglacial zone during 2002 (namely MLE and MLW, Table
122 1, Figure 1) are presented and discussed with regard to the impact subglacial processes may
123 have on the total runoff and solute budgets from the entire catchment. Meltwater samples
124 have been collected at these stream sites for major ion characterisation as part of an ongoing
125 monitoring programme that began in 1997 (Hodson et al. 2000; 2004; 2005a). On the glacier
126 surface, snowpack samples were collected using a depth-integrating 0.5 litre PVC tube
127 (Hodson et al. 2005a). Lysimeters of a similar design to those described in Hodson (2006),
128 were inserted into the base of the snowpack during summer 2003 to document the

hydrochemistry during snowpack ablation and major ion samples collected from one of the main supraglacial streams during 2003 (Figure 1) enabled solute characterisation of bulk supraglacial discharge.

All meltwater samples for major ion composition were filtered immediately in the field using a handheld Nalgene vacuum unit and 0.45µm cellulose nitrate filters to prevent further reaction with suspended sediment. Filters were pre-rinsed in the field using aliquots of sample water and field blanks have failed to indicate any potential contamination. Samples were stored airtight in pre-rinsed 60ml polyethylene Nalgene bottles (pre-rinsed with filtered sample water) and refrigerated to await further analysis. Snow samples were treated in the same manner as runoff samples after being melted in a 25 ^{o}C water bath (see Hodson et al. 2005a).

During 2002 and 2003 our geochemical sampling campaign was augmented by the determination of stable isotope ratios of $^{15}N/^{14}N$ and $^{18}O/^{16}O$ in NO_3^- and $^{15}N/^{14}N$ in NH_4^+. For the snowpack this involved collecting a c. 60 kg section of snow down to the glacier ice surface, in polyethylene bags, and for aqueous samples the collection of 20-40 L samples in polyethylene jerry cans. Details of sample processing are reported elsewhere (Wynn, 2004; Heaton et al. 2004; Wynn et al. 2006). The $^{15}N/^{14}N$ ratios of glacial till and fresh bedrock were determined on material from the glacier forefield. In the case of the glacial till, samples were collected from the immediate ice margin, representing young, former subglacial tills that have been exposed by the glacier's recent retreat. The rock samples included metamorphic basement rocks from the glacier's upper accumulation area (phyllite, schist, sandstones and quartzite) and younger sequences (chert) outcropping in the proximal parts of the glacier forefield.

Organic matter present within small melt pools known as cryoconite holes on the glacier surface was collected during summer 2002 and 2003 from three locations on the glacier surface and air-dried prior to analysis back in the UK.

2.2. Laboratory analysis

Anions of chloride and nitrate were determined using a Dionex DX100 ion chromatograph and soluble ammonium was analysed using a FOSS-Tecator FIAstar 5000 flow injection analyser. Based on repeat analysis of reference standard materials of comparable concentration to the samples being analysed, precision was calculated as 3.57, 1.16 and 2.54% RSD (relative standard deviation) for chloride, nitrate and ammonium respectively.

Snow, supraglacial and subglacial meltwaters collected for isotopic analysis were gravity-fed through cation and anion exchange resins, with nitrate processed to silver nitrate (Chang et al. 1999; Hwang et al. 1999; Silva et al. 2000; Heaton et al. 2004) and ammonium processed to ammonium sulphate (Sigman et al. 1997; Heaton, 2001).

2.3. Mass spectrometric analysis

Product silver nitrate, ammonium sulphate and cryoconite organic matter was analysed using ThermoFinnigan elemental analysers linked to a Delta + XL continuous flow mass spectrometer. Reductive pyrolysis of silver nitrate at 1400°C yielded CO and N_2 for determination of $^{18}O/^{16}O$ and N/O ratios, and oxidative combustion of silver nitrate, ammonium sulphate or organic matter at 900°C yielded N_2 and CO_2 for determination of $^{15}N/^{14}N$ and C/N ratios. Yield of N_2 from organic matter samples was determined by comparison of sample peak area with those from known weights of acetanilide. Ratios were converted to $\delta^{18}O$ values versus VSMOW:

$$\delta^{18}O_{sample}, \text{ in ‰} = \{[(^{18}O/^{16}O)_{sample} / (^{18}O/^{16}O)_{VSMOW})] - 1\} \times 1000 \quad (1)$$

and $\delta^{15}N$ values versus atmospheric N_2:

$$\delta^{15}N_{sample}, \text{ in ‰} = \{[(^{15}N/^{14}N)_{sample} / (^{15}N/^{14}N)_{atmos})] - 1\} \times 1000 \quad (2)$$

by comparison with within-run laboratory standards calibrated against IAEA-N3 ($\delta^{18}O$ value = +25.6 ‰ versus VSMOW (IAEA, 2004)), or against IAEA-N1 ($\delta^{15}N$ value = +0.4 ‰ versus atmos. N_2 (IAEA, 2004)). Precision on replicates of within-run laboratory standards was typically better than ±0.7‰ for $\delta^{18}O$ and ±0.3‰ for $\delta^{15}N$ (1 SD).

191

192 *2.4. Correction of $\delta^{18}O_{NO3}$ for organic matter*

193 If $\delta^{15}N$ and $\delta^{18}O$ values of nitrate are to be used as indicators of provenance, the silver nitrate
194 samples must be pure, i.e. free from any potential N- or O-bearing contaminants (Kendal,
195 1998; Haberhauer and Blochberger, 1999; Heaton et al. 2004). We found this to be a major
196 problem in the case of contamination derived from dissolved organics in low ionic strength
197 samples from the glacier surface during the first field campaign (2002). The amount of
198 contaminant organic matter in the final silver nitrate was reduced, but not eliminated by use of
199 ISOLUTE® Env^+ resin during sample preparation. Analysis of this organic matter, eluted
200 from the Env^+ resins with methanol and dichloromethane, failed to detect significant amounts
201 of nitrogen, but indicated large proportions of oxygen with average $\delta^{18}O$ values of +22‰ (1
202 SD = 2.4, n = 16). During the 2003 field campaign, Amberlite® XAD-7 and ISOLUTE® Env^+
203 resins were placed upstream of the cation and anion exchange resins during sample
204 concentration, thereby screening the ion exchange resins from extensive organic matter
205 contamination.

206 The fractional contribution of organic contaminant oxygen to the total oxygen in an impure
207 silver nitrate sample, $f_{organic}$, may be calculated from the sample's measured atomic N/O ratio
208 ($(N/O)_{measured}$), assuming pure nitrate has a ratio of 0.33 and the organic contaminant a ratio of
209 0:
210
211 $$f_{organic} = 1 - [(N/O)_{measured}/0.33] \quad (3)$$
212
213 If $f_{organic}$ has a $\delta^{18}O$ value of +22 ‰, then the isotopic composition of the pure nitrate, $\delta^{18}O_{NO3}$,
214 may be calculated from that of the measured impure silver nitrate sample, $\delta^{18}O_{measured}$, from:
215
216 $$\delta^{18}O_{NO3} = (\delta^{18}O_{measured} - f_{organic} \cdot 22) / (1 - f_{organic}) \quad (4)$$
217
218 All $\delta^{18}O$-nitrate signatures quoted in the remainder of this paper represent values corrected for
219 organic oxygen in the above manner. Obviously we cannot be totally certain that the $\delta^{18}O$
220 value of the organic matter recovered from the Env^+ resin is identical to the value for the
221 organic matter contaminating the sample. However, the values we measured are within the

222 defined range for organic oxygen and we believe that any differences which do occur will be
223 small enough not to have a significant effect on the correction procedure.
224
225 *2.5. Geologic nitrogen analysis*
226 The term 'geologic nitrogen' is taken to represent nitrogen located within the surrounding
227 bedrock (Holloway et al. 1998; 1999; Holloway and Dahlgren, 2002). In sedimentary rocks
228 such 'geologic nitrogen' is derived predominantly from decomposed organic matter which
229 thermally degrades during diagenesis and substitutes for potassium in minerals such as illite,
230 muscovite, biotite, and feldspars, forming fixed ammonium in metamorphic and igneous
231 rocks (Mingram and Brauer, 1998). The total nitrogen content of whole rock samples was
232 therefore determined using a Hydrofluoric acid / sulphuric acid digest (Honma and Itihara,
233 1981; Haendel et al. 1986). Precise experimental procedures followed were adapted from
234 Bradley (1992) and resultant ammonium/sulphuric acid solution was processed to ammonium
235 sulphate by ammonium diffusion (Sigman et al. 1997; Heaton, 2001) and analysed for $\delta^{15}N$.
236 Measurement precision based on replicates of standards was typically better than ±0.3‰ for
237 $\delta^{15}N$ (1 S.D) whilst experimental precision based on the repeat analysis of rock samples was
238 <2‰ (1 S.D). Yield of N_2 was determined by comparison of sample peak area with those of
239 known weights of acetanilide and blank contamination from the combined digest and
240 ammonium diffusion procedure was calculated as 2.5µg N per analysis (n=12, 1 S.D = 0.75).
241
242 **3. Results**
243 Figure 2 depicts the bulk hydrochemical outputs from the glacier catchment in major
244 proglacial streams (MLE and MLW) and the subglacial runoff (MLSG) during the 2002
245 observation period. Time series of discharge, Cl^- and NO_3^- show the typical early season
246 development of the hydrological system from a period dominated by snowmelt to one of
247 icemelt, supplemented by the release of subglacial water. Data from 2003 are not shown
248 because the position of the subglacial upwelling changed during the season, leading to
249 complex time series.
250
251 Table 2 shows summary statistics of the ionic and isotopic composition of NO_3^- and NH_4^+ in
252 pre-melt snow, snowmelt, supraglacial runoff and subglacial runoff during initial and
253 principal flow phases. The sharp boundary between the initial and principal flow phases
254 occurred just prior to sample collection on DOYs 184 and 193 during 2002 and 2003
255 respectively and is described in detail by Wynn et al. (2006).

256

257 During 2002, average NO_3^- concentrations in pre-melt snow, were 1.6μM. Concentrations of
258 NO_3^- in the subglacial waters of the principal runoff phase increased markedly to ca. 4 μM
259 and represent concentrations much greater than those observed during the initial runoff phase
260 (average 1.12 μM). During 2003, a strong elution phase produced very high average NO_3^-
261 concentrations in snowmelt relative to the pre-melt snowpack. However, concentrations of
262 NO_3^- were still greater in subglacial runoff of the principal runoff phase than the initial runoff
263 phase, although the effect was smaller than in 2002.
264

265 Average NH_4^+ concentrations were greatest in the pre-melt snowpack and snowmelt,
266 especially in 2003, (5.1 and 4.6 μM respectively), but lower in supraglacial streams (2.0 μM
267 in 2003), and subglacial runoff (0.17 μM at first, then 0.13 μM). In direct contrast to NO_3^-,
268 average NH_4^+ concentrations were lowest in subglacial runoff during the principal runoff
269 phase (Table 2). Table 2 also shows NO_3^-/Cl^- ratios for all sample types and mean $\delta^{15}N$ and
270 $\delta^{18}O$ values for NO_3^- in pre-melt snow, supraglacial runoff and subglacial meltwater. The
271 NO_3^-/Cl^- ratios were 0.015 in the pre-melt snowpack during 2002, whilst subglacial waters
272 showed average ratios that were lower during the initial flow phase (ca. 0.009), and markedly
273 higher during the principal runoff phase (0.038). During 2003, NO_3^-/Cl^- ratios in the
274 subglacial runoff during the initial runoff phase ($NO_3^-/Cl^- = 0.028$) were similar to those
275 reported in supraglacial samples, although higher ratios did appear during the principal runoff
276 phase ($NO_3^-/Cl^- = 0.056$). Therefore NO_3^-/Cl^- ratios in subglacial runoff show a clear tendency
277 to increase across the boundary of the initial and principal flow phases.
278

279 The isotope values in Table 2 and depicted in Figures 3 and 4 show significant differences
280 between sample types. Nitrate in pre-melt snow has low $\delta^{15}N$ values (-9.9 ‰ and -9.8 ‰ for
281 summer 2002 and 2003 respectively) and high $\delta^{18}O$ values (+57 ‰ to +72 ‰); the subglacial
282 waters of the principal runoff phase have higher $\delta^{15}N$ (-5.5 ‰ to –4.5 ‰) and lower $\delta^{18}O$
283 (+20 ‰), whilst subglacial waters during the initial flow phase have the highest $\delta^{15}N$ values
284 (+2.3 ‰ to +4.0 ‰) (Figures 3 and 4). For ammonium there was no clear distinction between
285 different samples, with all $\delta^{15}N$ values in the range of –6 ‰ to –2 ‰.
286

287 Geologic nitrogen concentrations and $\delta^{15}N$ signatures for rocks collected from the catchment
288 are given in Table 3. Concentrations of nitrogen were greatest in the phyllite, a major rock

289 type in the subglacial system, and pyritic chert, which lies amongst the chert sequences
290 beneath the lower ablation area of the glacier and its forefield. Phyllite and chert also
291 demonstrated the highest organic carbon contents (0.11 to 0.29 %). With the exception of the
292 low $\delta^{15}N$ value for the pyritic chert, which is a minor component of the chert, all other rock
293 types had $\delta^{15}N$ in the range +4.8 ‰ to +7.7 ‰.
294
295 Table 4 shows the $\delta^{15}N$ signature, N content and C/N ratio of the cryoconite organic matter
296 sampled during the two field campaigns. Nitrogen contents are at least an order of magnitude
297 greater than those recovered in the rock samples owing to the abundance of micro-algae,
298 bacteria, viruses and a number of other microorganisms in these active microbial habitats
299 (Säwström et al. 2002).
300
301 **4. Discussion**
302 *4.1. Hydrochemical regime*
303 The hydrochemical regime of Midtre Lovénbreen during the 2002 summer melt season is
304 depicted in Figure 2. A steady increase in discharge in both the bulk meltwater proglacial
305 streams began when the glacier was completely snow covered on DOY 168. At MLE,
306 discharge continued to rise after DOY 182 due to the subglacial outburst, whilst discharge
307 driven principally by icemelt stabilised at MLW. By the end of the observation period shown
308 in Figure 2, icemelt was dominating runoff production across the entire glacier, although
309 snowmelt continued to emerge from the subglacial upwelling due to runoff from the
310 accumulation area entering the subglacial drainage system through stable crevasses and
311 moulins at approximately 400m altitude (Irvine-Fynn et al. 2005). The persistent input of
312 snowmelt is indicated by the high Cl^- in waters marked MLSG in Figure 2, whilst more dilute
313 Cl^- concentrations rapidly appear at MLE and MLW when icemelt dominates runoff delivery
314 to other flowpaths (i.e. supraglacial streams and lateral channels: cf Tranter et al. 1996). The
315 decline in Cl^- concentrations at MLE and MLW therefore reflects this dilution. However, they
316 also reflect the elution mechanism that removes solute rapidly from the snowpack, which
317 explains why Cl^- concentrations also gradually decline in the subglacial runoff (Tranter et al.
318 1996; Wadham et al. 1998). This elution process also appears to have governed changes in
319 NO_3^- in the proglacial rivers, because these too show a significant decline prior to the
320 emergence of subglacial runoff. Concentrations of NO_3^- then increase disproportionately
321 compared to Cl^- in the MLE stream two days after the emergence of the subglacial runoff.

The two day delay in increasing NO_3^- concentrations was likely caused by the displacement of "old" subglacial water during the initial flow phase. This component of the subglacial runoff was depleted in both oxygen and NO_3^- prior to the transition to the principal runoff phase (Wynn et al. 2006).

Later in the principal runoff phase, the subglacial drainage system developed an efficient, channelised configuration that conveyed runoff with residence times of just 2-4 hours following descent into moulins in the uppermost part of the glacier (Irvine-Fynn et al. 2005). During this phase, runoff via the subglacial upwelling increased to ca. 25 – 33 % of the total catchment runoff (Hodson et al. 2005b). Intuitively, one would therefore expect the proportion of atmospheric-derived NO_3^- (i.e. snow pack NO_3^-) transported by the subglacial river to dominate during this period. However, the following characteristics confound this interpretation and require an alternative explanation:

1) High NO_3^-/Cl^- ratios and NO_3^- concentrations develop in subglacial runoff relative to all other streams flowing at the same time and to subglacial runoff during the initial flow phase earlier in the summer (Figure 2, Table 3);

2) At the same time, the subglacial runoff nitrate displays higher $\delta^{15}N$ values and lower $\delta^{18}O$ values than the snowpack and supraglacial streams.

Waters from the initial flow phase, when subglacial runoff is dominated via delayed flow pathways, have lower NO_3^- concentrations and NO_3^-/Cl^- ratios due to denitrification (Wynn et al. 2006). Thus their mixing with surface-derived meltwaters would reduce the NO_3^- levels of subglacial runoff relative to surface melt waters – which is opposite to the observed pattern (Table 2). An alternative source of NO_3^-, with higher $\delta^{15}N$ and lower $\delta^{18}O$ values than those of the surface runoff, must be added to these supraglacial meltwaters during their passage through the glacier.

4.2. Nitrification as a mechanism for additional NO_3^- production

Nitrification has been invoked as a source of NO_3^- in a number of glacial and periglacial environments without actually being observed directly. For example, very significant excess NO_3^- production in two cold-based glacier basins has been proposed by Hodson et al. (2005a) and Hodson (2006). Further, studies of talus waters within rock glaciers have identified high

354 NO_3^- waters that are also thought to betray bacterial activity and nitrification (Bieber et al.
355 1998). However, two studies have failed to stimulate nitrification in supraglacial snowpacks
356 amended with NH_4^+ (Williams et al. 1996; Wynn, Unpublished Data), suggesting that the
357 process takes place in alternative environments. The possibility that nitrification takes place at
358 the bed of Midtre Lovénbreen is therefore considered below using $\delta^{18}O_{NO3-}$ data from 2003.
359
360 The microbial nitrification of ammonia utilises both H_2O and O_2 as the source of oxygen
361 during the production of NO_3^-. On the basis that two thirds of the oxygen molecules are
362 sourced from H_2O and the remainder obtained from atmospheric O_2 (Kumar et al. 1983;
363 Anderson and Hooper, 1983), it has been proposed that the expected $\delta^{18}O$ value for
364 microbially-produced nitrate can be calculated (Equation 5) (eg. Amberger and Schmidt,
365 1987; Kendall, 1998; Mayer et al. 2001).
366
367 $$\delta^{18}O_{NO3} = (0.33 \times \delta^{18}O_{Air}) + (0.66 \times \delta^{18}O_{water}) \quad (5)$$
368
369 As the average $\delta^{18}O_{water}$ value of the subglacial discharge during the principal flow phase was
370 -12.3‰ (Table 2), and assuming $\delta^{18}O_{Air}$ = +23.7 ‰ (value for atmospheric O_2; Horibe, et al.
371 1973), the theoretically expected $\delta^{18}O_{NO3}$ value for microbially produced nitrate is -0.3 ‰.
372 Taking an average $\delta^{18}O_{NO3}$ value for snow to be +64 ‰, a mixture of 68 % microbial nitrate
373 plus 32 % snowmelt nitrate would produce the $\delta^{18}O_{NO3}$ value of +20.3 ‰, similar to the value
374 for NO_3^- observed in the 2003 principal subglacial runoff phase (20.3 ‰ ± 6.1 ‰ (1 S.D)). As
375 there is no isotopic evidence for the presence of microbially mediated nitrate in the lysimeter
376 melt waters and supraglacial streams (average $\delta^{18}O_{NO3}$ = +63.8 ‰), these data therefore imply
377 that microbial nitrification must be occurring within or at the bed of the glacier, accounting
378 for much of the nitrate present in subglacial runoff during the principal runoff phase. Using
379 these same proportions for nitrate from snow and microbial sources, we can then estimate the
380 $\delta^{15}N_{NO3}$ value of the microbial nitrate. Thus, if the subglacial nitrate outflow during the
381 principal runoff phase, ($\delta^{15}N_{NO3}$ value = –5.5 ‰ in 2003: Table 2) was made up of 32 %
382 snowmelt nitrate with a $\delta^{15}N_{NO3}$ value between -9.8 ‰ and –7.8 ‰ (range for snow and
383 supraglacial waters), then the 68 % of nitrate sourced from microbial activity in the 2003
384 subglacial runoff would have had a $\delta^{15}N_{NO3}$ value of –4.4 ‰ to –3.5 ‰.
385
386 *4.3. Potential NH_4^+ sources for nitrification*

Given the above, the following potential sources of nitrogen might be driving a nitrification process:

1) NH_4^+ from snowpack and glacier ice;

2) Rock-derived NH_4^+ liberated following dissolution reactions; and

3) Biologically-derived NH_4^+ produced following mineralisation of organic N.

Given that the NH_4^+ abundance in this glacial environment is low (Table 2), a negligible fractionation effect is likely during the nitrification process (Fogel and Ciffuentes, 1993; Kendall, 1998; Heaton, 1986). We would therefore expect the $\delta^{15}N_{NH4+}$ value of the ammonium to be very similar to the average product $\delta^{15}N_{NO3-}$ of ca. –4.4 ‰ to –3.5 ‰. Snowpack NH_4^+ has already been constrained by our measurements ($\delta^{15}N_{NH4+}$ of -1.7 ‰ $\pm$ 1.6 ‰ in 2002 to -2.8 ‰ in 2003: Table 2) and appears slightly higher than what is required if the NO_3^- were derived from nitrification of this source. Bulk snowmelt $\delta^{15}N_{NH4}$ values sampled from the lysimeters were lower than the snowpack composition ($\delta^{15}N_{NH4+}$ of -5.2 ‰ during summer 2003) and thus closer to the principal phase subglacial runoff $\delta^{15}N_{NO3-}$ and $\delta^{15}N_{NH4+}$ values observed during summer 2003. The difference between the high parent snowpack $\delta^{15}N_{NH4+}$ value and the low lysimeter and supraglacial stream runoff values is unclear. However, it is also uncertain on account of just one snowpack sample being available for 2003. We therefore believe that the larger data sets used to constrain the isotopic composition of snowmelt in the lysimeters (n = 8) and mixtures of snowmelt and supraglacial streams (n = 6) provide the best indication of surface inputs to the subglacial drainage system during the principal runoff phase.

In contrast to the supraglacial samples described above, rock $\delta^{15}N$ values were far higher than the snowpack and stream samples, being +7.2 ‰ for phyllite, the most dominant N-containing rock type beneath the glacier, and +7.7 ‰ for subglacial till. It therefore appears that the nitrification of ammonia within crushed rock and glacial till beneath the glacier is unlikely to furnish a product $\delta^{15}N_{NO3-}$ composition of ca. –4.4 ‰ to –3.5 ‰ unless there are very significant fractionation effects during the mineral dissolution process. Presently there are no data with which to assess the magnitude of such effects.

During the overall conversion of organic nitrogen to nitrate, mineralization represents the rate determining step when the size of the ammonium substrate pool is small (Equation 6) (Heaton, 1986).

$$\text{Organic-N} \xrightarrow[\text{mineralisation}]{} NH_4^+ \xrightarrow[\text{nitrification}]{} NO_2^- \rightarrow NO_3^- \quad (6)$$

Under these conditions, we would again expect the nitrate formed from the mineralization and nitrification of organic N to have a δ^{15}N-value very similar to that of the source organic matter. Organic material lies upon the glacier surface in cryoconite holes, characterised by an organic N content of 1 to 2 mg/g and C/N ratios (10.6 to 11.7) typical of microbial matter (Takeuchi et al, 2002). Importantly, since cryoconite holes cover up to 6% of the glacier surface (Hodson et al. 2005a) they offer much potential for ammonia assimilation into the organic phase and subsequent mineralisation. Further, the ^{15}N values observed for organic matter (-3 to -5 ‰) (Table 4) lie closer to the inferred product $\delta^{15}N_{NO3-}$ range of –4.4 ‰ to –3.5 ‰ than any of the other potential sources (ie other pathways of nitrification from surface melt and rocks).The mineralization of surface derived microbial organic matter transported to the glacier bed may thus provide a reliable source of NH_4^+ for nitrification in addition to the NH_4^+ contained within snow melt and supraglacial runoff. However, since their isotopic compositions are very similar, no further distinctions can be made using isotopic data and we instead use time series of NO_3^- production inferred from our ionic data.

4.4. Temporal dynamics of NO_3^- production and NH_4^+ loss

Our observations suggest that nitrification of NH_4^+ in the glacial catchment is significant following the onset of snowmelt, a finding that is commensurate with the ammonia loss identified in catchment-scale annual mass balances presented by Hodson et al. (2005a) and Wynn (2004). Here we use the 2002 major ion data set to establish the seasonal (sub-annual) dynamics of NO_3^- production and NH_4^+ loss in proglacial streamflow. The terms $^{excess}NO_3^-$ and $^{deficit}NH_4^+$ are defined in the following manner:

$$^{excess}NO_3^- = {}^{total}NO_3^- - (0.021Cl^-) \quad (7)$$

$$^{deficit}NH_4^+ = {}^{total}NH_4^+ - (0.014Cl^-) \quad (8)$$

The constants 0.021 and 0.014 represent the average NO_3^-/Cl^- and NH_4^+/Cl^- ratios respectively (in μM) in 2002 lysimeter melt waters, and thus enable removal of snowmelt NO_3^- and NH_4^+ under the assumption that Cl^- is a conservative tracer of snowmelt. We used the lysimeter data, rather than bulk snowpack data, because the number of pre-melt snow samples was too

small (see Table 2) and because the ratios could then be estimated using a wide range of solute concentrations similar to those observed in the streams. Our ratios were not influenced by preferential elution effects, because time series of NO_3^-/Cl^- ratios in supraglacial streams do not indicate that the process occurs on the glacier surface.

Figure 5 shows time series of the $^{deficit}NH_4^+$ and $^{excess}NO_3^-$ at MLE, MLW and in the initial and principal phases of subglacial runoff during 2002. Concentrations of dissolved Si are also shown to indicate the presence of waters from high rock-water contact environments (no Si could be detected in snowmelt). Prior to DOY 173 streamflow was dominated by runoff from the glacier forefield and margins. During this time $^{excess}NO_3^-$ was negative at MLW and coincident with high dissolved silica concentrations suggesting meltwater passage through low redox environments conducive to denitrification in the proglacial sediments. Subsequent to DOY 173, $^{excess}NO_3^-$ values remained remain close to zero for the remainder of the ablation season at MLW, thereby providing no evidence of NO_3^- production in the western parts of the glacier, its margins and forefield during 2002. In contrast, significant $^{excess}NO_3^-$ levels at MLE were co-incident with the emergence of subglacial meltwaters on DOY 184, indicating a major input of NO_3^- that cannot be accounted for by the delayed release of concentrated snowpack waters. The first fractions of subglacial outflow during the initial flow phase carried a distinct signature of negative $^{excess}NO_3^-$ associated with denitrification (see Wynn et al. 2006). Maximum $^{excess}NO_3^-$ occurred on DOY 187 and for the rest of the monitoring period $^{excess}NO_3^-$ concentrations remain stable, as do dissolved silica levels. Subglacial runoff is therefore responsible for all $^{excess}NO_3^-$ in the stream at MLE, as $^{excess}NO_3^-$ concentrations here were negligible prior to DOY 184.

Figure 5 also shows that the $^{deficit}NH_4^+$ was greatest at the start of the ablation period, implying that catchment-wide loss of ammonium is greatest when the snowpack is isothermal and begins to produce runoff. The $^{deficit}NH_4^+$ was identical at MLE and MLW prior to DOY 184, suggesting rates of ammonium loss might be uniform across the catchment during the early ablation period. However, the release of subglacial runoff on DOY 184 (the start of the principal flow phase) coincided with the release of very NH_4^+-deficient runoff from beneath the glacier, suggesting snowpack-derived NH_4^+ is very likely to undergo nitrification within the subglacial environment.

Table 5 shows estimates of Cl^-, NH_4^+, NO_3^-, $^{excess}NO_3^-$ and $^{deficit}NH_4^+$ mass fluxes for the main rivers shown in Figure 1. The fluxes have been estimated from the product of daily discharge and concentration pairs, using linear interpolation to fill any gaps in the latter series. These data show that for subglacial runoff, NO_3^- production (i.e. the $^{excess}NO_3^-$ flux) exceeded NH_4^+ loss (the $^{deficit}NH_4^+$ flux) during 2002. These mass balance calculations therefore suggest that the nitrification of snow and icemelt NH_4^+ only explained 83 % of the excess NO_3^-, suggesting that an additional substrate for $^{excess}NO_3^-$ production within the subglacial environment must also exist. Isotope data suggest the mineralisation of surface-derived organic matter is the most likely source. However, when all rivers are considered, the mass balance calculations show that the $^{deficit}NH_4^+$ flux exceeds $^{excess}NO_3^-$ at the catchment scale. Thus it is very likely that ammonia assimilation into organic matter (most likely within cryoconite holes on the surface of the glacier) is important before streams enter the glacier and undergo ammonia loss through processes of nitrification.

The processes responsible for $^{excess}NO_3^-$ and $^{deficit}NH_4^+$ within the glacial system can thus be summarised as follows:

$^{excess}NO_3^-$ = nitrification of ammonia + mineralization and nitrification of Organic N

$^{deficit}NH_4^+$ = nitrification of ammonia + assimilation into organic matter

Mass flux calculations in Table 5 show that the $^{excess}NO_3^-$ flux in the principal subglacial runoff phase accounts for 100 % of its catchment-wide production and is equivalent to 25 % of the entire NO_3^- exported by the proglacial rivers. However, the total $^{deficit}NH_4^+$ is even more striking, implying an 82 % reduction in the total meltwater transport of NH_4^+ prior to leaving the catchment. In this particular year, the net effect is for NH_4^+ assimilation into the organic phase to reduce the export of dissolved inorganic nitrogen (i.e. DIN or $NO_3^- + NH_4^+$) by 27 %. These figures therefore serve to demonstrate the significant reactivity of DIN in the glacial ecosystem following the onset of melt.

5. Conclusions

The dissolved inorganic nitrogen content of glacial meltwaters, NO_3^-/Cl^- ratios and $\delta^{15}N$ and $\delta^{18}O$ isotopic ratios have been used to try to understand the capacity for glacial runoff to export NO_3^- fluxes that are in excess of those entering the catchment via atmospheric

deposition. In so doing, we have been able to characterise significant rates of NO_3^- production beneath a high Arctic glacier in Svalbard, European High Arctic. Our data show that much of the NO_3^- present within the subglacial meltwaters has most likely been produced following the microbial nitrification of snowpack NH_4^+ and mineralisation of organic nitrogen. Presently, we are unable to identify the exact substrate(s) used, due to similar $\delta^{15}N$ end member compositions. Mass fluxes indicate that loss of NH_4^+ is widespread across the entire glacier basin and often exceeds the excess nitrate produced in the subglacial environment. This suggests there must be an additional sink for ammonia within the catchment and is likely represented through the assimilation of ammonia into organic matter such as that contained within cryoconite holes on the surface of the glacier. Overall, NO_3^- production, which is responsible for enhancing the NO_3^- fluxes leaving the catchment by 25%, was far outweighed by NH_4^+ assimilation occurring elsewhere and causing an 82% reduction in the NH_4^+ content of runoff.

Acknowledgements

This work was supported by a Natural Environment Research Council studentship to P. Wynn; CASE industrial partnership funding in association with the NERC Isotope Geoscience Laboratory, British Geological Survey; and Royal Society 20th IGC funding to A. Hodson.

References

Amberger, A. and Schmidt, H.-L., 1987. Naturliche Isotopengehalte von Nitrat als Indikatoren fur dessen Herkunft. Geochimica et. Cosmochimica Acta, 51, 2699-2705

Andersson, K.K. and Hooper, A.B., 1983. O_2 and H_2O are each the source of one O in NO_2^- produced from NH_3 by Nitrosomanas: ^{15}N-NMR evidence. FEBS letters, 164 (2), 236-240

Bhatia, M., Sharp, M and Foght, J., 2006. Distinct microbial communities exist beneath a High Arctic polythermal Glacier. Applied and Environmental Microbiology, 72 (9), 5838-5849

Bieber, AJ., Williams, MW., Johnsson, MJ. and Davinroy, TC., 1998 Arctic and Alpine Research, 30 (3), 266-271

Copland, L., Sharp, M. and Nienow, P.W., 2003. Links between short-term velocity variations and the subglacial hydrology of a predominantly cold, polythermal glacier, Journal of Glaciology, 49 (166), 337-348

Bingham, R.G., Nienow, P.W., Sharp, M.J and Copland, L. 2006. Hydrology and dynamics of a polythermal (mostly cold) High Arctic glacier. Earth Surface Processes and Landforms, 31, 1463-1479

Bottrell, S.H. and Tranter, M., 2002. Sulphide oxidation under partly anoxic conditions at the bed of Haut Glacier D'Arolla, Switzerland. Hydrological Processes, 16 (12), 2363-2368

576 Bradley, A.D., 1992. Collection, preparation and analysis of NH_4-1: A standard reference
577 material for ammonium determination. British Geological Survey Technical Report,
578 Analytical Geochemistry Series, WI/92/3
579
580 Brown, G.H., Tranter, M and Sharp, M.J., 1996. Experimental investigations of the
581 weathering of suspended sediment by alpine glacial melt water. Hydrological Processes, 10,
582 579-597
583
584 Caulkett, A.P. and Ellis-Evans, J.C., 1997. Chemistry of streams of Signy Island, maritime
585 Antarctic: sources of major ions. Antarctic Science, 9 (1), 3-11
586
587 Chang, C.C.Y., Langston, J., Riggs, M., Campbell, D.H., Silva, S.R and Kendall, C., 1999. A
588 method for nitrate collection for $\delta^{15}N$ and $\delta^{18}O$ analysis from waters with low nitrate
589 concentrations. *Canadian Journal of Fisheries and Aquatic Science,* 56, 1856–1864
590
591 Fogel, M.L. and Cifuentes, L.A., 1993 Isotope fractionation during primary production. *In*:
592 Engel, M.H. and Macko, S.A. (eds.) *Organic Geochemistry*, Plenum Press, New York
593
594 Foght, J., Aislabie, J., Turner, S., Brown, C.E., Ryburn, J., Saul, D.J. and Lawson, W., 2004.
595 Culturable bacteria in subglacial sediments and ice from two Southern Hemisphere glaciers.
596 Microbial ecology, 47 (4) 329-340
597
598 Haberhauer, G. and Blochberger, K., 1999. A simple cleanup method for the isolation of
599 nitrate from natural water samples for O isotope analysis. Analytical Chemistry, 71 (16),
600 3587-3590
601

602 Haendel, D., Mühle, K., Nitzsche, H-M., Stiehl, G. and Wand, U., 1986. Isotopic variations of
603 the fixed nitrogen in metamorphic rocks. Geochimica et Cosmochimica Acta, 50, 749-758
604
605 Heaton, T.H.E., Wynn, P.M. and Tye, A., 2004. Low $^{15}N/^{14}N$ ratios for nitrate in snow in the
606 High Arctic (79°N). Atmospheric environment, 38, 5611-5621
607
608 Heaton, T.H.E., 2001. Procedure and notes on the 'diffusion' method for 15N/14N analysis of
609 nitrate and ammonium. NERC Isotope Geosciences Laboratory, Report NIGL 176, 5pp
610
611 Heaton, T. H. E., 1986. Isotopic studies of nitrogen pollution in the hydrosphere and
612 atmosphere: a review. *Chemical Geology,* 59, 87-102
613
614 Hjelle, A., 1993. *Geology of Svalbard*. Norsk Polarinstitutt, Oslo
615
616 Hodson, A., Tranter, M. and Vatne, G., 2000 Contemporary rates of chemical denudation and
617 atmospheric CO_2 sequestration in glacier basins: An Arctic perspective. Earth Surface
618 Processes and Landforms*,* 25, 1447–1471
619
620 Hodson, A.J., Mumford, P.N. and Lister, D., 2004. Suspended sediment and phosphorous in
621 proglacial rivers: bioavailability and potential impacts upon the P status of ice-marginal
622 receiving waters. *Hydrological Processes*, 18, 2409-2422
623
624 Hodson, A.J., Mumford, P.N., Kohler, J. and Wynn, P.M., 2005a. The High Arctic glacial
625 ecosystem: new insights from nutrient budgets. Biogeochemistry, 72, 233-256
626

627 Hodson, A.J., Kohler, J. and Brinkhaus, M., 2005b Multi-year water and surface energy
628 budget of a high latitude polythermal glacier: evidence for overwinter water storage in a
629 dynamic subglacial reservoir. Annals of glaciology, 42 (1), 42-46
630
631 Hodson, A., 2006. Biogeochemistry of snowmelt in an Antarctic glacial ecosystem. Water
632 Resources Research, 42, W11406. DOI: 10.1029/2005WR004311
633
634 Hodson, A.J., Anesio, A. M., Tranter, M., Fountain, A., Osborn, M., Priscu, J., Laybourne-
635 Parry, J. and Sattler, B. Glacial Ecosystems. Ecological Monographs, In Press
636
637 Holloway, J. M., Dahlgren, R. A., Hansen, B. and Casey, W. H., 1998. Contribution of
638 bedrock nitrogen to high nitrate concentrations in stream water. Nature, 395, 785-788
639
640 Holloway, J. M. and Dahlgren, R.A., 1999. Geological nitrogen in terrestrial biogeochemical
641 cycling. Geology, 27, 567-570
642
643 Holloway, J. M. and Dahlgren, R.A., 2002. Nitrogen in rock: Occurrences and
644 biogeochemical implications Global biogeochemical cycles, 16 (4), 1-17
645
646 Honma, H. and Itihara, Y., 1981. Distribution of ammonium in minerals of metamorphic and
647 granitic rocks. Geochimica et Cosmochimica Acta, 45, 983-988
648
649 Horibe, Y., Shigehara, K. and Takakuwa, Y., 1973. Isotope separation factor in carbon
650 dioxide-water system and isotopic composition of atmospheric oxygen. Journal of
651 Geophysical Research, 78, 2625-2629

652

653 Hwang, H.-H., Liu, C.-L.J., Hackley, K.C., 1999. Method improvement for oxygen isotope
654 analysis in nitrates. Geological Society of America Abstracts with programs, North-Central
655 Section, 31, p. A-23 No. 5, April 22-23, Champaign, Il
656
657 Irvine-Fynn, T.D.L., Hodson, A.J., Kohler, J., Porter, P. and Vatne, G.,
658 2005. Dye tracing experiments at Midtre Lovénbreen, Svalbard: preliminary results and
659 interpretations, In: Mavlyudov, B.R. (ed.): Proceedings of the 7th Glacier Caves and Glacial
660 Karst in High Mountains and Polar Regions, Institute of the Russian Academy of Sciences,
661 Moscow, 36 – 43.
662
663 IAEA., 2004. Reference materials catalogue 2004-2005, Analytical Quality Control Services,
664 International Atomic Energy Agency, Vienna
665
666 Kendall, C., 1998. Tracing nitrogen sources and cycling in catchments. *In*: Kendall, C. and
667 McDonnell, J.J. (eds.) *Isotope tracers in catchment hydrology*, Amsterdam, Elsevier Science,
668 B.V.
669
670 Kumar, S., Nicholas, D.J.D. and Williams, E.H., 1983. Definitive 15N NMR evidence that
671 water serves as a source of 'O' during nitrite oxidation by Nitrobacter agilis. FEBS Letters,
672 152 (1), 71-74
673
674 Mader, H.M., Pettitt, M.E., Wadham.J.L., Wolff, E.W., Parkes, R.J., 2006. Subsurface ice as a
675 microbial habitat. Geology, 34 (3), 169-172
676
677 Mayer, B., Bollwerk, S.M., Mansfeldt, T., Hütter. and Veizer, J., 2001. The oxygen isotope
678 composition of nitrate generated by nitrification in acid forest floors. Geochimica et
679 Cosmochimica Acta, 65 (16), 2743-2756

Mingram, B. and Brauer, K., 2001. Ammonium concentration and nitrogen isotope composition in meta-sedimentary rocks from different tectonmetamorphic units of the European Variscan Belt. Geochimica et Cosmochimica Acta, 65 (2), 273-287

Nutall, A-M. and Hodgkins, R., 2005. Temporal variations in flow velocity at Finsterwalderbreen, a Svalbard surge-type glacier. Annals of Glaciology, 42 (1), 71-76

Nienow, P.W., Sharp, M.J and Willis, I.C., 1998. Seasonal changes in the morphology of the subglacial drainage system, Haut Glacier D'Arolla, Switzerland. Earth Surface processes and Landforms, 23, 825–843

Raiswell, R., 1984 Chemical models of solute acquisition in glacial meltwaters. Journal of Glaciology, 30 (104), 49-57

Richards, K., Sharp, M., Arnold, N., Gurnell, A., Clark, M., Tranter, M., Nienow, P., Brown, G., Willis, I. and Lawson, W., 1996. An integrated approach to modelling hydrology and water quality in glacierized catchments. Hydrological processes, 10, 479-508

Rippin, D., Willis, I., Arnold, N., Hodson, A.J., Moore, J., Kohler, J. and Björnsson, H., 2003. Changes in geometry and subglacial drainage of Midtre Lovénbreen, Svalbard, determined from digital elevation models. Earth Surface Processes and Landforms, 28, 273-298

Rippin, D.M., Willis, I.C., Arnold, N.S., Hodson, A.J and Brinkhaus, M., 2005. Spatial and temporal variations in surface velocity and basal drag across the tongue of the polythermal glacier Midtre Lovénbreen, Svalbard. Journal of Glaciology, 51 (175), 588-600

707 Säwström, C., Mumford, P., Marshall, W., Hodson, A.J. and Laybourn-Parry, J., 2002. The
708 microbial communities and primary productivity of cryoconite holes on an Arctic glacier
709 (Svalbard, 79ºN). Polar Biology, 25 (8), 591-596
710
711 Sharp, M., Tranter, M., Brown, G.H. and Skidmore, M., 1995. Rates of chemical denudation
712 and CO_2 drawdown in a glacier-covered Alpine catchment. Geology, 23, 61-64
713
714 Sharp, M., Parkes, J., Cragg, B., Fairchild, I.J., Lamb, H. and Tranter, M., 1999. Widespread
715 bacterial populations at glacier beds and their relationship to rock weathering and carbon
716 cycling. Geology, 27 (2), 107-110
717
718 Sigman, D.M., Altabet, M.A., Michener, R., McCorkle, D.C., Fry, B and Holmes, R.M.,
719 1997. Natural abundance-level measurement of the nitrogen isotopic composition of oceanic
720 nitrate: an adaption of the ammonia diffusion method. Marine Chemistry, 57, 227-242
721
722 Silva, S. R., Kendall, C., Wilkison, D. H., Ziegler, A. C., Chang, C. C. Y. and Avanzino, R.
723 J., 2000. A new method for collection of nitrate from freshwater and the analysis of nitrogen
724 and oxygen isotope ratios. Journal of Hydrology, 228, 22-36
725
726 Skidmore, M., Foght, J.M. and Sharp, M., 2000. Microbial Life Beneath a High Arctic
727 Glacier. Applied and Environmental Microbiology, 66 (8), 3214-3220
728
729 Takeuchi, N., 2002. Optical characteristics of cryoconite (surface dust) on glaciers: the
730 relationship between light absorbency and the property of organic matter contained in the
731 cryoconite. Annals of Glaciology, 34, 409-414

732

733 Tranter, M., Brown, G., Raiswell, R., Sharp, M. and Gurnell, A., 1993. A conceptual model of
734 solute acquisition by Alpine glacial meltwaters Journal of Glaciology, 39 (133), 573-581

735

736 Tranter, M., Brown, G.H., Hodson, A., Gurnell, A.M. and Sharp, M.J., 1994. Variations in the
737 nitrate concentration of glacial runoff in Alpine and sub-polar environments. IAHS
738 Publication, 223, 299-311

739

740 Tranter, M., Brown, G.H., Hodson, A., Gurnell, A.M., 1996 Hydrochemistry as an indicator
741 of the nature of subglacial drainage system structure: a comparison of Arctic and Antarctic
742 environments. Hydrological Processes, 10, 541-556

743

744 Tranter, M., Sharp, M.J., Brown, G.H., Willis, I.C., Hubbard, B.P., Nielson, M.K., Smart,
745 C.C., Gordon, S., Tulley, M. and Lamb, H.R., 1997. Variability in the chemical composition
746 of *in situ* subglacial meltwaters. Hydrological Processes, 11, 59-77

747

748 Tranter, M., Skidmore, M and Wadham, J., 2005. Hydrological controls on microbial
749 communities in subglacial environments. Hydrological Processes, 19, 995-998

750

751 Tockner, K., Malard, F., Uchlinger, U and Ward, J.V., 2002. Nutrients and organic matter in a
752 glacial river-floodplain system (Val-Roseg, Switzerland). Limnol. Oceanogr., 47 (1), 266-277

753

754 Wadham, J.L., Hodson, A.J., Tranter, M. and Dowdeswell, J.A., 1998. The hydrochemistry of
755 meltwaters draining a polythermal-based high Arctic glacier, South Svalbard: I. The ablation
756 season. Hydrological Processes, 12, 1825-1849

757

758 Wadham, J.L., Bottrell, S., Tranter, M. and Raiswell, R., 2004. Stable isotope evidence for
759 microbial sulphate reduction at the bed of a polythermal high Arctic glacier. Earth and
760 Planetary Science Letters, 219, 341-355

Welker, J.M., Fahnestock, J.T., Henry, G.H.R., O'Dea, K.W. and Piper, R.E., 2002. Microbial activity discovered in previously ice-entombed arctic ecosystems. Eos, 83 (26), 281-282

Williams, M. W., Brookes, P. D., Mosier, A. and Tonnessen, K., 1996. Mineral nitrogen transformations in and under seasonal snow in a high-elevation catchment in the rocky mountains, United States. Water resources research, 32 (10), 3161–3171

Wynn, P., Hodson, A.J. and Heaton, T.H.E., 2006. Chemical and isotopic switching within the subglacial environment of a high arctic glacier. Biogeochemistry, 78, 173-193

Wynn, P., 2004. The provenance and fate of nitrogen in arctic glacial meltwaters: an isotopic approach. Unpublished Ph.D thesis, University of Sheffield

787 **Figure 1:** Location map and sampling sites of Midtre Lovénbreen, Svalbard

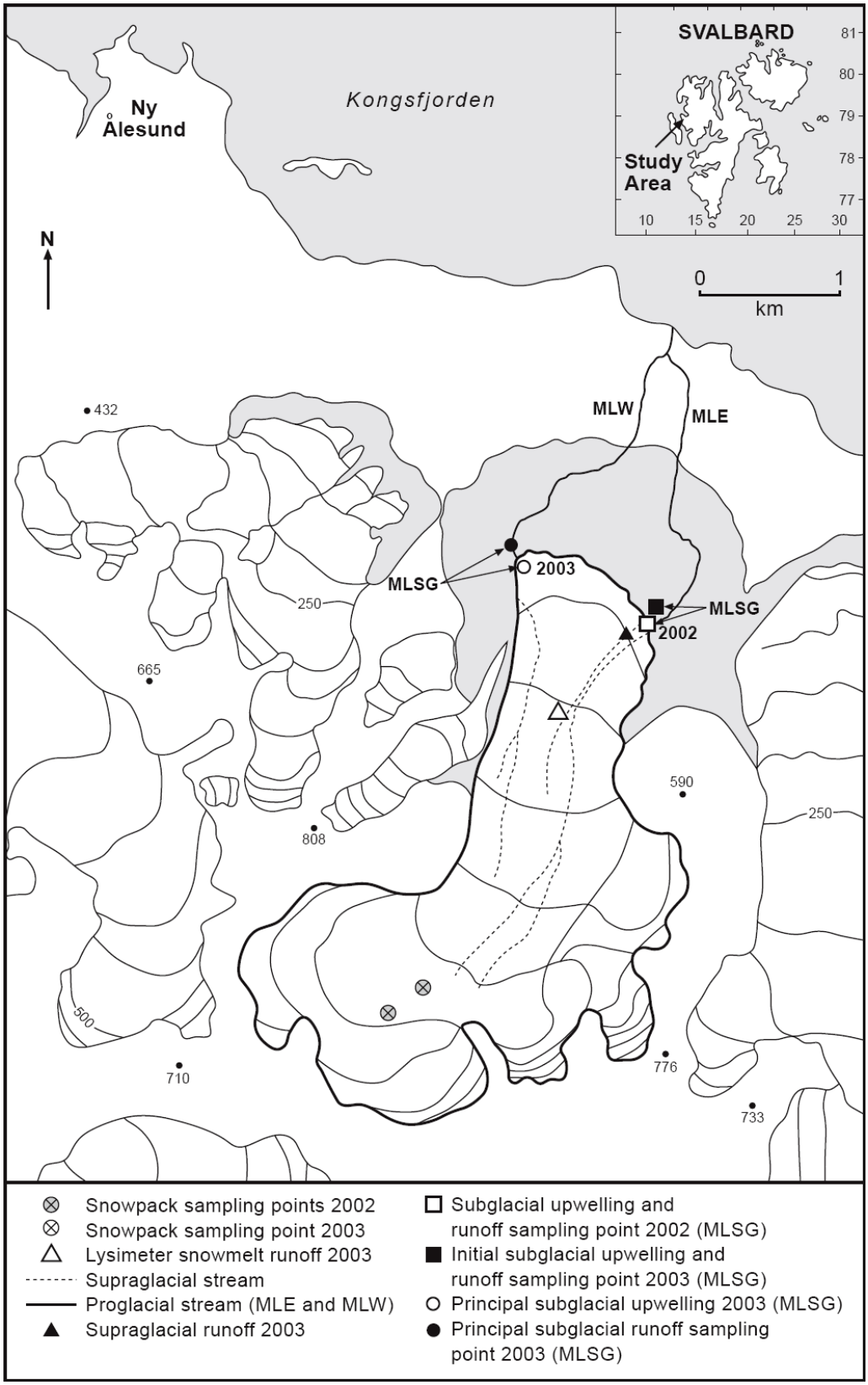

788

789 **Figure 2.** Time series of bulk hydrochemical outputs from the glacier catchment in major
790 proglacial streams (MLE, MLW and MLSG) for a) discharge b) chloride and c) nitrate
791 concentrations during the 2002 observation period

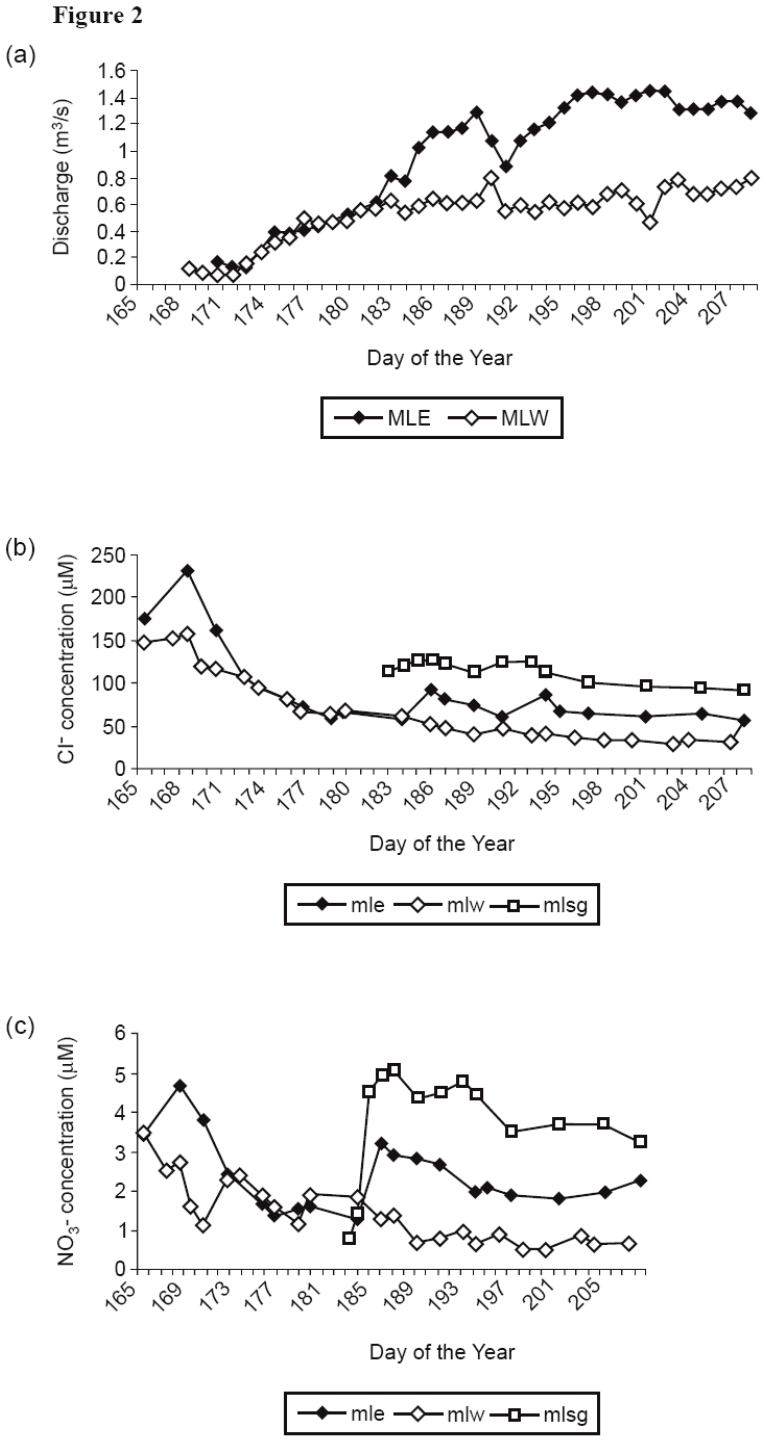

792

793 **Figure 3.** $\delta^{15}N$ values of nitrate in pre-melt snow and subglacial meltwater

794

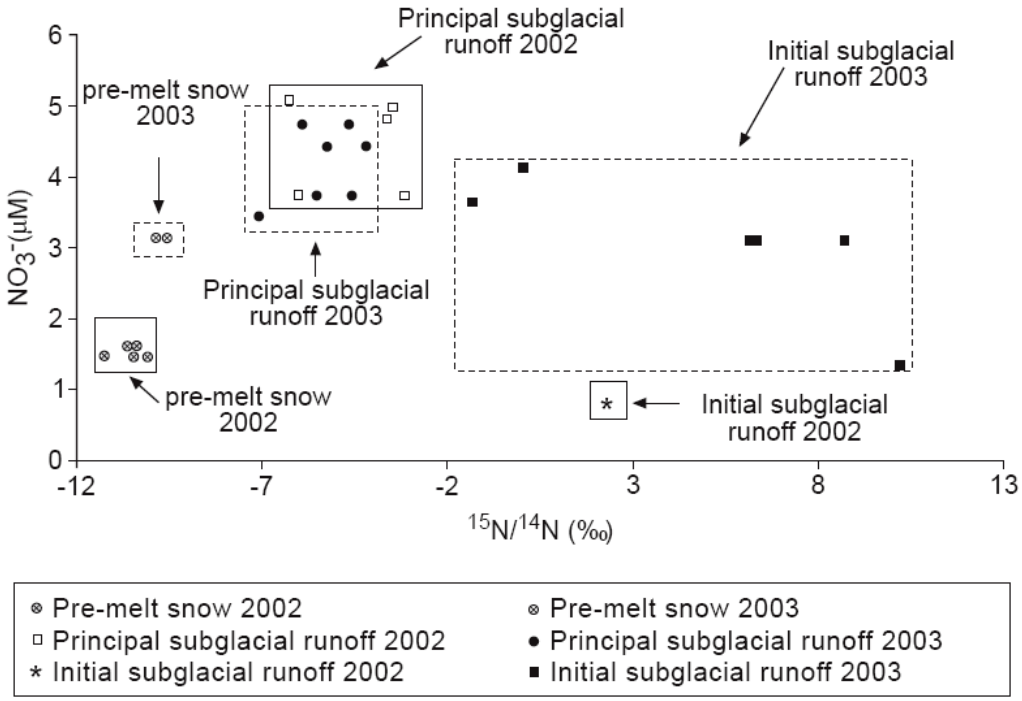

795

796

797

798

799

800

801

802

803

804

805

806

807

Figure 4: $\delta^{18}O$ values of nitrate in pre-melt snow and subglacial meltwater

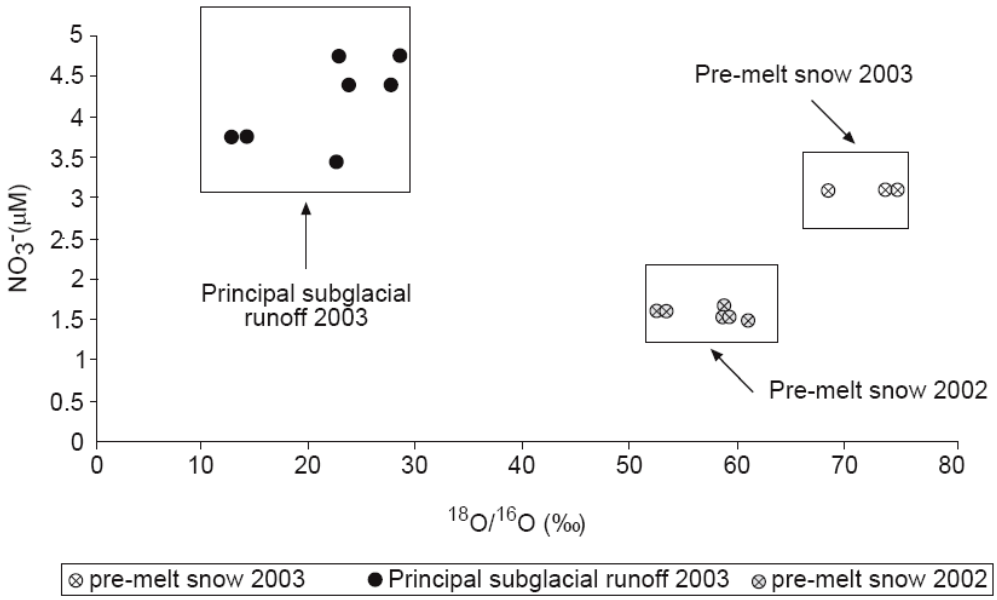

824 **Figure 5:** Time series of a) excess nitrate b) deficit ammonium and c) silica concentrations in
825 major proglacial streams (MLE, MLW and MLSG) during the 2002 observation period

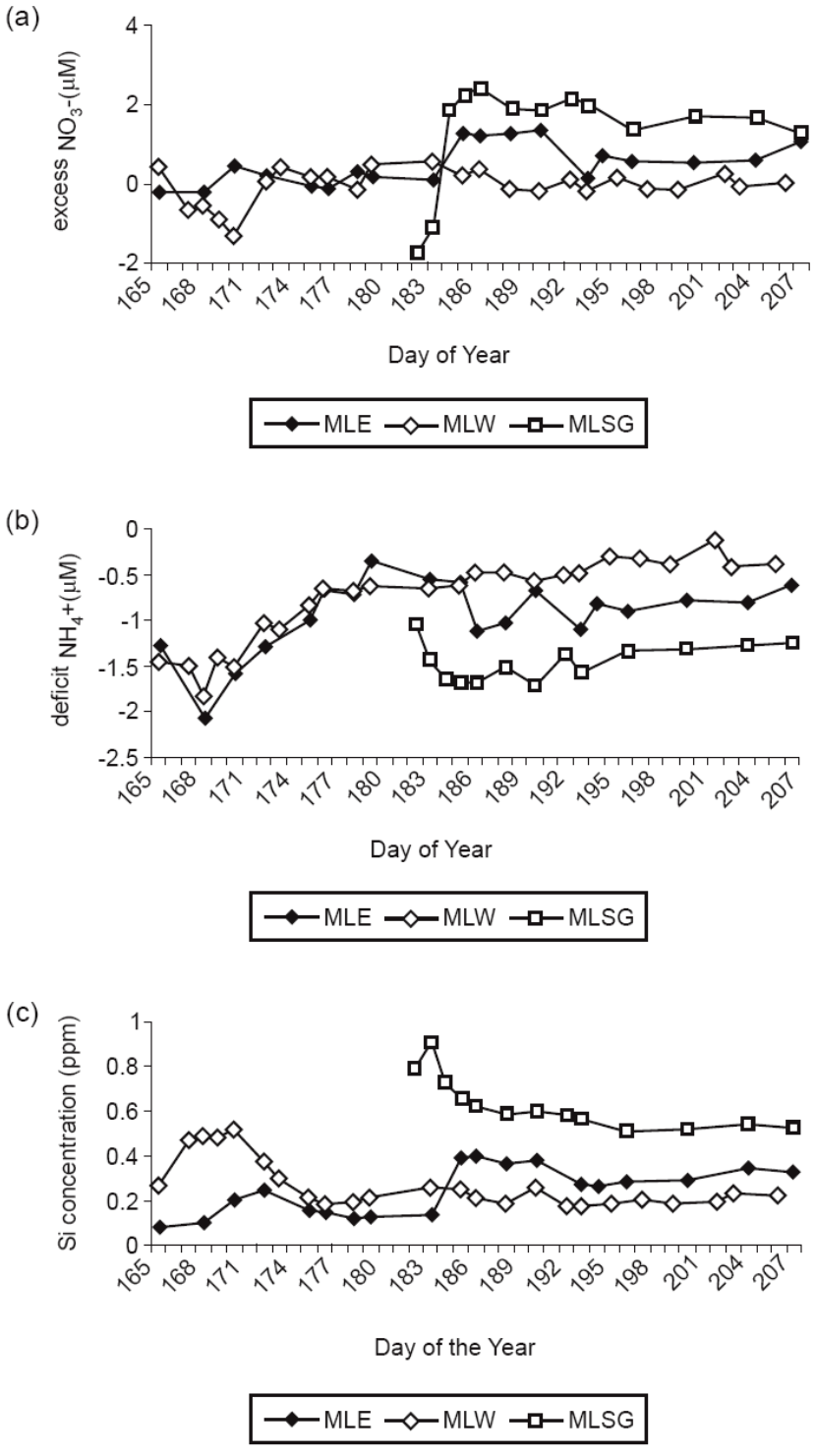

826

827 **Tables**

828 **Table 1:** Hydrological components sampled at Midtre Lovénbreen during summer 2002 and

829 2003

Sampling location	Abbreviation in text	Active monitoring period (DOY)	Description of water type
Pre-melt snowpack 2002	-----	101-102	Winter accumulation unaffected by summer ablation
Pre-melt snowpack 2003	-----	164	Winter accumulation unaffected by summer ablation
Lysimeter snowmelt 2002	-----	173-189	Snowmelt collected prior to contact with glacier ice
Lysimeter snowmelt 2003	-----	167-178	Snowmelt collected prior to contact with glacier ice
Supraglacial runoff 2003	-----	175-203	Bulk snowmelt and glacier ice
Subglacial runoff, initial runoff phase, 2002	MLSG	182-183	Sub-oxic discharge of long residence time and high rock-water contact. Sampled directly from upwelling on eastern side of glacier margin
Subglacial runoff: principal runoff phase, 2002	MLSG	184 onwards	Aerated subglacial discharge of low residence time. Sampled directly from upwelling on eastern side of glacier margin
Subglacial runoff, initial runoff phase, 2003	MLSG	186-193	Sub-oxic discharge of long residence time and high rock-water contact. Sampled directly from upwelling on eastern side of glacier margin
Subglacial runoff, principal runoff phase, 2003	MLSG	193 onwards	Aerated subglacial discharge of low residence time. Sampled downstream from upwelling on western side of glacier margin as mixture of supraglacial and subglacial water.
Midtre Lovénbreen East proglacial stream 2002	MLE	168-207	Bulk supraglacial and subglacial runoff plus groundwater component from proglacial zone
Midtre Lovénbreen West proglacial stream 2002	MLW	168-207	Bulk supraglacial runoff plus groundwater component from proglacial zone

830
831
832
833
834
835
836
837
838
839
840
841
842
843
844

Table 2: Nitrogen chemistry for pre-melt snow, supraglacial and subglacial meltwater samples from Midtre Lovénbreen

	n^* =	NO_3^- (µmol/l)	NH_4^+ (µmol/l)	NH_4^+:Cl^- (µmol/l)	NO_3^-:Cl^- (µmol/l)	$\delta^{15}N\text{-}_{NO3}$* (‰)	$\delta^{18}O\text{-}_{NO3}$* (‰)	$\delta^{15}N\text{-}_{NH4}$* (‰)	$\delta^{18}O\text{-}_{H2O}$* (‰)
Surface water									
Pre-melt snow 2002	$n^1 = 2$ $n^2 = 2$	1.6 (0.1)	0.97 (0.1)	0.009 (0.001)	0.015 (0.0001)	-9.9 (0.02)	+57.3 (2.7)	-1.7 (1.6)	-12.41
Pre-melt snow 2003	$n^1 = 1$ $n^2 = 1$	3.1	5.1	0.04	0.027	-9.8	+72.0	-2.8	-11.94
Lysimeter snowmelt 2002 (DOY 173 – 189)	$n^1 = 8$	1.4 (0.7)	1.14 (1.37)	0.014 (0.012)	0.21 (0.017)	-----	-----	-----	-----
Lysimeter snowmelt 2003 (DOY 167 – 178)	$n^1 = 9$ $n^2 = 8$	5.7 (7.0)	4.6 (3.4)	0.067 (0.036)	0.047 (0.0078)	-8.6 (0.7)	+64.5 (2.8)	-5.2 (0.2)	-12.73 (0.79)
Supraglacial streams 2003	$n^1 = 8$ $n^2 = 6$	1.9 (2.0)	2.0 (1.7)	0.02 (0.02)	0.029 (0.017)	-7.8 (2.20)	+63.1 (3.81)	-5.8 (1.0)	-11.68 (0.85)
Subglacial, initial runoff phase									
2002 DOY 182-183	$n^1 = 2$ $n^2 = 1$	1.1 (0.50)	0.52 (0.30)	0.004 (0.002)	0.0094 (0.0036)	+2.3	-----	-2.0	-12.46
2003 DOY 186-193	$n^1 = 8$ $n^2 = 4$	3.0 (1.0)	0.17 (0.08)	0.001 (0.0007)	0.028 (0.0084)	+4.0 (5.5)	-----	-6.1 (1.5)	-12.27
Subglacial, principal runoff phase									
2002 DOY 184 onwards	$n^1 = 11$ $n^2 = 4$	4.3 (0.6)	0.14 (0.10)	0.0009 (0.0008)	0.038 (0.002)	-4.5 (1.3)	-----	-2.9 (2.7)	-12.59
2003 DOY 193 onwards	$n^1 = 8$ $n^2 = 4$	3.9 (0. 6)	0.13 (0.20)	0.001 (0.002)	0.059 (0.0031)	-5.5 (1.1)	+20.3 (6.1)	-5.8 (3.5)	-11.61

*n represents the number of field samples. n^1 represents the number of major ion samples collected. n^2 represents the number of isotope samples collected. 1SD is given in parentheses.

Table 3: Analysis of geological specimens from the Midtre Lovénbreen catchment for $\delta^{15}N\text{-}NH_4^+$ and nitrogen concentration

Rock type	NH_4^+-N (µg/g)	$\delta^{15}N_{-NH4+}$ * (‰) Vs AIR	Replication (1 SD) (‰)	Organic Carbon (%)
Phyllite	198	+7.2	0.18 (*n*=3)	0.29
Green Chert	59.3	+4.8	2.00 (*n*=2)	0.11
Pyritic Chert	168	-1.6	---	No data
Subglacial till	52.0	+7.7	0.37 (*n*=2)	0.06
Green schist	0.00	Below detection	---	0.03
Basement carbonates	6.06	Below detection	---	0.03
Sandstone	13.2	+4.8	---	No data
quartz	0.23	Below detection	---	0.03

Table 4: Nitrogen composition of cryoconite organic matter

	n =	$\delta^{15}N$ (‰)	N content (mg/g)	C/N ratio
Cryoconite organic matter 2002	3	-4.8 (0.31)	1.2 (1.0-1.4)	11.4 (11.05-11.63)
Cryoconite organic matter 2003	6	-3.3 (0.83)	1.9 (1.8-2.0)	11.3 (10.6-11.7)

Values in parentheses represent one standard deviation for isotopes and ranges for all other data.

Table 5: Molar flux estimates during the 2002 observation period

	$^{excess}NO_3$ (M)	$^{deficit}NH_4$ (M)	Total NO_3 (M)	Total NH_4 (M)	Cl (M)
East proglacial stream (MLE)	2170	-2700	6990	560	230000
West proglacial stream (MLW)	130	-990	2090	270	91000
Total Catchment	2300	-3690	9070	830	323000
Total subglacial runoff (MLSG)	2300	-1900	5350	140	148000
Subglacial delivery ratio	1.00	0.52	0.59	0.16	0.46